Proceedings of ERAD 2006

Modelling of radar echoes from rain by a physically-based simulator

Carlo Capsoni[1], Roberto Nebuloni[2]

[1]Politecnico di Milano, Milan (Italy).

[2] Istituto di Elettronica e Ingegneria Informatica e delle Telecomunicazioni, CNR, Milan (Italy).

1 Introduction

Nowadays, multiparameter meteorological radar are largely used because of their ability to supply different independent measurements of the target section (Doviak and Zrnić (1993)). This, in turn, allows a more accurate identification of the target nature and a more reliable quantification of its backscatter cross.

It is well known that in order to obtain meaningful results, radar measurements must be carried out according to specific rules. This requirement is even more strict for polarimetric measurements: a non accurate estimation of their values reflects usually in large discrepancies of the meteorological quantities of interest (e.g. rain intensity). Moreover, when polarimetric measurements are used to infer the nature of the ensemble of scatterers in the resolution volume, high accuracy of the measurements is needed (Bringi and Chandrasekar (2001)).

The complexity and multiplicity of meteorological phenomena in the atmosphere acting on the scatterers make sometimes quite complex their identification also through a set of polarimetric measurements. In this respect, it is very useful to have the support of theoretical computations that give the guidelines for the interpretation of the radar outputs. Unfortunately, only in few relatively simple cases the analytical approach can be used after assumptions and approximations. An alternative is the use of a software radar simulator of the physical type, i.e. one able to reproduce the interaction of a radar beam with the population of hydrometeors subjected to different kind of actions from the surrounding environment.

Correspondence to: Roberto Nebuloni

nebuloni@elet.polimi.it

This paper is intended to present the effects of drop shape and drop oscillations on the estimates of a number of radar observables, including copolar and differential reflectivity.

2 The radar simulator

The physically-based radar simulator used in this study is an upgraded version of the one presented in Capsoni et al. (2001). For sake of clarity its characteristics are summarized in the following. The meteorological environment is modelled by a population of falling hydrometeors (of different nature, physical state, size, shape and orientation), subjected to the action of the gravitational force and wind. The sensor is described through the antenna pattern, the frequency of operation, the pulse duration, the Pulse Repetition Time (PRT) and the so-called range-weighting function. The synthetic pulse-echo signal reproduces the in-phase and quadrature components at the output of a coherent receiver for each of two orthogonal linear polarizations.

With respect to the version in Capsoni et al. (2001), the simulator has been upgraded with a more accurate description of the meteorological environment: the (large) volume enclosed by the antenna beam width from the radar to the resolution cell is subdivided in boxes (parallepipeds), which size is defined by the user, according to the type of meteorological situation to be simulated. Each box is filled with a population of randomly distributed hydrometeors in a given physical state and with equivalent rain intensity R. Because it is not possible to manage the actual number of drops per unit volume, a compression algorithm reduces this number to a minimum while preserving the spectral content of the signal. According to the drop-size distribution (DSD) and the value of R selected, the program assigns a weight to each one of the size bins the DSD is divided into. These input parameters can be defined independently for each box. In this way, it is possible to simulate precipitation gradients or the contemporaneous presence of bright band and rain within the resolution cell. Further, because the space is subdivided into small volumes, the simulator takes properly into account the effect of path propagation, i.e. extra attenuation and phase shift introduced by the hydrometeors along the path.

Once the environment has been generated, hydrometeors in each box are left to fall down with their natural vertical velocity and to oscillate (in the case of raindrops), with or

without the superimposed effect of wind. While falling, hydrometeors move from one box to the other in a continuum-like medium. When a particle exits the lowest box, it is replaced by another particle of equal size. The new scatterer is placed in a random position in the highest box and at a random time within a PRT. Finally, at each PRT, a sample of the return echo is "received" by the polarimetric radar and stored for further processing. Contributions due to noise and clutter can be superimposed to the precipitation echo with predetermined power ratios (i.e. S/N, S/C or S/(N+C)).

3 Model of drop oscillations

As shown by various authors, drops in their trajectory towards the ground do not maintain the equilibrium shape but tend to oscillate. Feng and Beard (1991) developed a perturbation model of raindrop oscillations which includes aerodynamic effects using the method of multiple moments. They show that the oscillation modes can be either axisymmetric, when a two-sided scatter between oblate-prolate shapes around the equilibrium shape is observed, or asymmetric, i.e. one-side variations of the axis ratio. At present, models resulting from fit of laboratory data or outdoor measurements are available. Here we refer to one introduced by Beard and Kubesh (1991) for the case of axisymmetric oscillation, which describes the time varying axis ratio as

$$\frac{b(t)}{a(t)} = \frac{a_0 + A\sin\omega t}{a_0 - 0.5A\sin\omega t} \qquad (1)$$

where $a(t)$ and $b(t)$ are the major and minor axes of the spheroid, A represents the oscillation amplitude and ω is 2π times the oscillation frequency, which ranges from few hundreds of Hz for small drops to few tens of Hz for larger drops. This oscillation mode has been observed during a recent experiment aimed to measure drop shape using a 2D video disdrometer (Thurai and Bringi (2005)). The resulting axis ratio distributions were found to be Gaussian in shape with standard deviation increasing with drop diameter, and mean value close to the one given by Beard and Chuang (1987). The mean drop axis ratio and its distribution around the mean value, are reported here for convenience in Table 1 after Thurai and Bringi (2005).

In order to reproduce correctly the physical process, the number of raindrops per bin size (that is, per diameter interval of the DSD) has been properly increased at the very beginning of the simulation. Each set of drops with the same size is initialized so that the corresponding axis ratios b/a are randomly distributed between the $\pm 3\sigma$ limits of the normal distribution in Table 1. Then drops are left to fall with their axis ratio varying according to Eq. (1) at the frequency of oscillation given by the theoretical formula $\omega = C\,D^{-3/2}$ where C is a constant and D is the drop diameter (Beard and Kubesh (1991)). If the shape of drops changes at each PRT, the backscatter cross section correspondingly changes, hence it has to be updated every time. To reduce the computational effort, the simulator makes use of analytical interpolating functions of the backscatter cross section of each drop diameter.

Table 1. Mean and standard deviation of Gaussian functions fitted to the deconvolved axis ratio distributions after Thurai and Bringi (2005).

Diameter interval (cm)	Mean axis ratio	Std dev.
1.0-1.5	0.980	0.036
1.5-2.0	0.948	0.037
2.0-2.5	0.911	0.028
2.5-3.0	0.881	0.031
3.0-3.5	0.844	0.037
3.5-4.0	0.808	0.050
4.0-4.5	0.771	0.073
4.5-5.0	0.732	0.081
5.0-5.5	0.704	0.077
5.5-6.0	0.671	0.071
6.0-6.5	0.645	0.072
6.5-7.0	0.617	0.071
7.0-7.5	0.586	0.075
7.5-8.0	0.553	0.068
8.0-8.5	0.520	0.070
8.5-9.0	0.476	0.065

4 Results

The simulations aim to check the effect of oscillating drops on the estimate of both reflectivity (Z_{HH} and Z_{VV}) and differential reflectivity Z_{DR}. The parameters of the simulations are listed in Table 2. The virtual drops in the resolution cell are about 2×10^4 . As the DSD is discretized into 300 size bins, each bin contains (on the average) several tens of particles, which are necessary to reproduce the statistical fluctuations of the signal when drops oscillate. On the contrary, in the absence of oscillations few drops per class would be enough to simulate the random process.

Fig. 1 shows Z_{HH} , Z_{VV} and Z_{DR} as a function of the rain rate for the two cases of stable (i.e. non-oscillating) and oscillating drops, respectively. The difference in magnitude between the corresponding curves is of the order of 0.6 dB for Z_{HH} and 0.8 dB for Z_{VV}. If the above differences are expressed in terms of rain rate, it turns out that neglecting oscillations produces a small overestimation if Z_{HH} is used and a small underestimation if Z_{VV} is used (up to about 10% in both cases). The discrepancy in Z_{DR} between the use of a

stable raindrop model and a model that takes into account oscillations can be quantified in at least a 0.25 dB overestimation in the former case that increases to 0.5 dB for R > 5 mm/h and 1 dB for R > 40 mm/h . At this intensity level the stable drop model gives roughly twice the Z_{DR} of the dynamic drop model.

Table 2. Parameters used in the simulations

Frequency	2.8 GHz (S-band)
Beam width	2º
Range resolution	75 m
Elevation angle	3º
Resolution cell distance	10 km
DSD	Marshall-Palmer
Equilibrium shape of drops	Oblate spheroid
Oscillation mode	Axisymmetric oblate-prolate

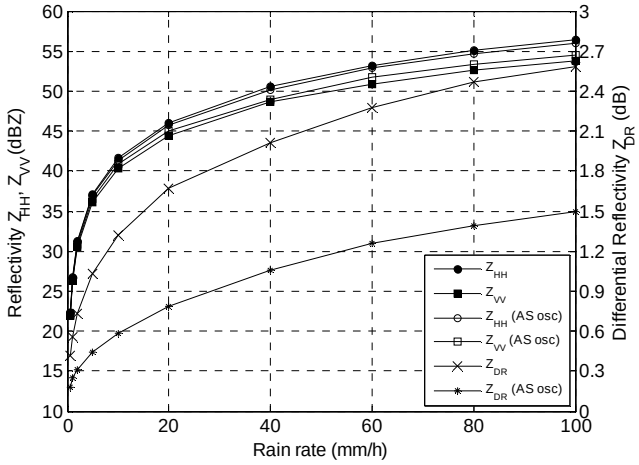

Fig. 1. Copolar reflectivity and differential reflectivity at S-band against rain rate for stable drops and oscillating drops in the axisymmetric (AS) mode.

The above differences result from the variations in the backscatter cross section of the particles. In fact, if we consider the set of drops with diameter D, the symmetrical Gaussian distribution of axis ratios of oscillating drops turns into an asymmetrical distribution of the backscatter cross section, as shown in the normal probability plot of Fig 2. The cross sections in the graph are normalized to zero mean value and unit standard deviation.

In Fig. 3 we plot the uncertainty of reflectivity estimates expressed in dB against the number of independent samples. For a better interpretation of graphs, the reader should recall the following rule of thumb (Sachidananda and Zrnić (1985)): a 1 dB standard deviation in Z_{HH} (or Z_{VV}) or a 0.1 dB standard deviation in Z_{DR} lead to a 25% error in rain rate estimates. From inspection of Fig. 3. we conclude that drop oscillations have a negligible effect on the precision of copolar reflectivity estimates while the uncertainty of Z_{DR} increases at low rain rates.

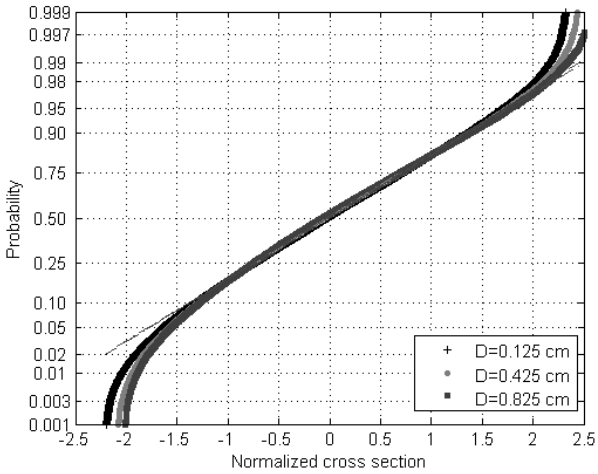

Fig. 2. Normal probability plot of the normalized backscatter cross section of oscillating drops at S-band for three different drop diameters D. Straight dash-dot lines are for normal distributions.

Finally Fig. 4 shows how the copolar correlation coefficient $|\rho_{HV}(0)|$ changes when drop oscillations are considered in the simulations. $|\rho_{HV}(0)|$ measures the correlation of the backscattering complex amplitudes along two orthogonal axes (Zrnić et al. (1994)). As for previous Fig. 1 the curves have been obtained generating a large number of independent samples, i.e. they represent asymptotic estimates. There is a reduction in $|\rho_{HV}(0)|$ because both the oscillation frequency and the oscillation amplitude depend on size, hence the two field components scattered from the population of particles do not vary in unison. However, the difference between non-oscillating and oscillating drops is limited and generally overshadowed by the statistical fluctuations of $|\rho_{HV}(0)|$ measurements, which are generally based on a limited number of independent samples.

5 Conclusions

A physically-based radar simulator has been used to illustrate the effect of raindrop oscillations on conventional and polarimetric radar observables. Simulations show that a simple model with a unique axisymmetric oblate-prolate mode of oscillation results in small differences of copolar reflectivity estimates, while variations in the differential reflectivity are noticeable. As a consequence, the estimation of rainfall by both Z_{HH} and Z_{DR} is critical not only because of the intrinsic sensitivity of Z_{DR} to measurement errors, but also because of its sensitivity to raindrop oscillations. However, a definitive answer about the effect of oscillations

on radar observables has yet to be given, as the phenomenon has not been fully investigated.

References

Beard K. V. and R.J. Kubesh, 1991: Laboratory measurements of small raindrop distortion. Part II: Oscillation frequencies and modes. *J. Atmos. Sci*., **48**, 2245-2264.

Beard K. V., and C. Chuang, 1987: A new model for the equilibrium shape of raindrops, *J Atmos. Sci*., **44**, 1509-1524.

Bringi V. N. and V. Chandrasekar, 2001: *Polarimetric Doppler weather radar*, Cambridge University Press, Cambridge UK.

Capsoni, C., M. D'Amico, and R. Nebuloni, 2001: A multiparameter polarimetric radar simulator. *J. Atmos.Oceanic Technol.*, **18**, 1799-1809.

Doviak R. J., and D. S. Zrnić, 1993: *Doppler Radar and Weather Observations*, 2nd edition, Academic Press, San Diego CA.

Feng, J. Q. and K. V. Beard, 1991: A perturbation model of raindrop oscillation characteristics with aerodynamic effects, *J. Atmos. Sci*., **49**, 1856-1868.

Sachidananda, M. and D. S. Zrnić, 1985: ZDR measurement considerations for a fast scan capability radar, *Radio Sci*., **20**, 907–922.

Thurai, M. and V. N. Bringi, 2005: Drop axis ratios from 2D video disdrometer, *J. Atmos.Oceanic Technol*, **22**, 966-978.

Zrnić, D. S., N. Balakrishnan, A. V. Ryzhkov, and S. L. Durden, 1994: Use of copolar correlation coefficient for probing precipitation at nearly vertical incidence, *IEEE Trans. Geosci. Remote Sens.*, **32**, 740-748.

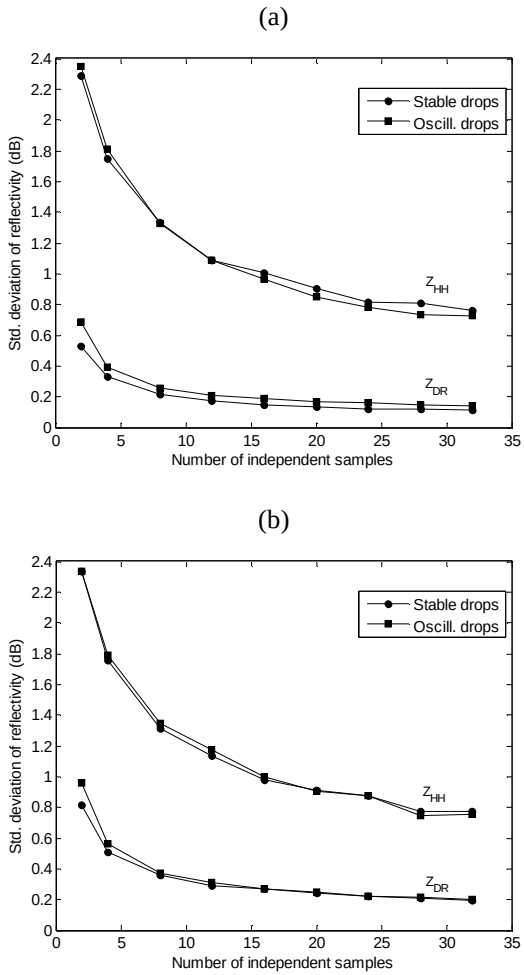

Fig. 3. Standard deviation of copolar reflectivity and differential reflectivity (at S-band) as a function of the number of independent samples for stable drops and oscillating drops. The rain rate is 1 mm/h in (a) and 100 mm/h in (b), respectively.

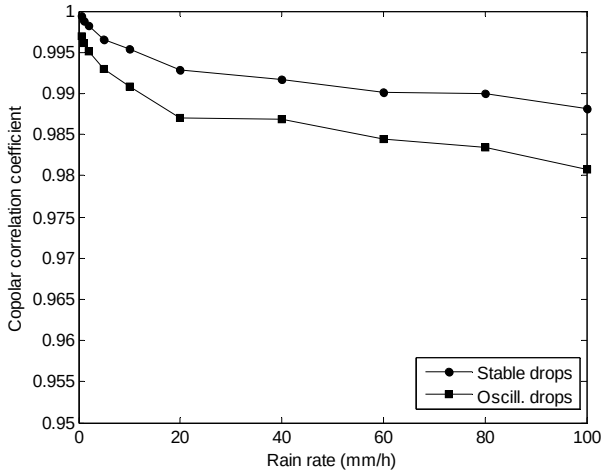

Fig. 4. Copolar correlation coefficient at S-band against rain rate for stable drops and oscillating drops in the axisymmetric mode.